Quantitative Assessment of Background Field Removal Methods for Abdominal Imaging

Debra E. Horng[1,2], Samir D. Sharma[1], Diego Hernando[1], and Scott B. Reeder[1,2]
[1]*Radiology, University of Wisconsin-Madison, Madison, WI, United States,* [2]*Medical Physics, University of Wisconsin-Madison, Madison, WI, United States*

Target audience: Researchers interested in QSM (quantitative susceptibility mapping).

Purpose: Accurate susceptibility estimation with QSM requires background field removal, preceding (or in combination with[1]) dipole inversion. Since QSM had initially been developed for brain applications, it is unknown whether current background field removal algorithms perform accurately in the abdomen. For example, in the liver, iron deposits are spatially diffuse, occur in high concentrations, and lie close to the lungs. The ***purpose of this work*** is to assess the accuracy of previously described background field removal algorithms (PDF[2] and SHARP[3]) in the context of abdominal imaging.

Methods: **Phantom:** A phantom was created out of a large pure water bath (42cm×30.2cm×17.8cm) containing either ***(1)*** a large polypropylene vial (cylinder of diameter 6.0cm and height 7.3cm) or ***(2)*** a small polypropylene vial (cylinder of diameter 1.6 cm and height 15cm). The large vial was used to simulate a diffuse distribution of iron within the liver, and the small vial was used to simulate a concentrated iron deposit within the brain. Multiple concentrations of diluted gadobenate dimeglumine (MultiHance, Bracco Diagnostics, Princeton, NJ) were used in both sizes of vials: 1, 2, 3, and 4% MultiHance (diluted by volume), corresponding to calculated susceptibilities of -7.3, -5.6, -3.9, and -2.1 (SI volume susceptibility at 20°C, relative to water at -9.02 ppm). These concentrations were chosen to mimic the susceptibility of iron-overloaded liver[4].

Acquisition: The vials were scanned at both central (closer to the center of the bath) and edge (closer to the edge of the bath, i.e. closer to the air) locations (see Fig. 1). The central location was used to simulate the deep iron deposits of the brain, and edge location was used to simulate the liver dome that is close to the lungs. A baseline water vial scan was acquired for each contrast vial scan, as an estimate of the background field from the contrast vial scan.

The phantoms were scanned on a 1.5T system (Signa HDxt, GE Healthcare, Waukesha, WI USA), using an 8-channel coil, a multi-echo 3D SPGR sequence, and no parallel imaging. Scan parameters included: FOV=41 cm, slice thickness=2.5mm, 56 slices, matrix=224×224, TE1=1.5ms, ΔTE=2.6ms, TR=16.6ms, 6 echoes/TR, and flip angle=5°.

Processing: The scan data were reconstructed at a resolution of 1.6mm×1.6mm×2.5mm. Echo images were input to a signal model, producing a water signal and a field map (see Fig. 2). The 'true local field' was calculated by the subtraction of the contrast agent vial field map and the baseline water vial field map (see Fig. 3). The field map from the contrast agent scan (the 'total field') was input into two widely-used background field removal algorithms, PDF and SHARP, to obtain an estimate of the local field.

Performance comparison: The results of each algorithm were compared to the true local field by the error per voxel (E_L) defined on a 3D ROI: $E_L=\|f_L-\hat{f}_L\|_2/N$, where f_L=true local field, $\hat{f}_L$=local field estimate, and N=number of voxels in the ROI. The 3D ROI was chosen in each exam to be a cylindrical region centered on the vial, and twice its diameter.

Results: The errors (Hz/voxel) for PDF and SHARP are shown in Figure 4. Factors that increase errors in background field removal are smaller vial size, increasing contrast agent concentration, and a closer position to air. Both PDF and SHARP have relatively small errors per voxel: less than 0.5 Hz per voxel difference from the true local field.

Discussion and Conclusion: We have assessed the performance of background field removal techniques in the context of abdominal imaging. Error analysis suggests that both the high concentrations of iron in the liver, and the liver's proximity to the lungs will lead to larger errors. However, the diffuse distribution of liver iron reduces this error. Quantitative assessment of background field removal may be used to improve existing algorithms or aid in the development of novel algorithms for liver QSM.

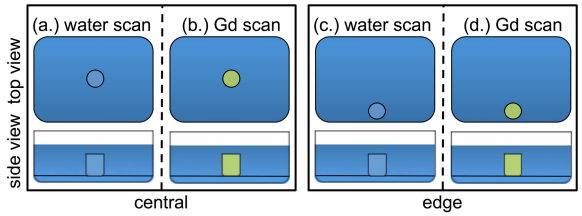

Figure 1. Each contrast agent scan was paired with a baseline water scan. All concentrations were scanned at both central (a.-b.) and edge (c.-d.) locations for both large (6 cm diameter) and small (1.6 cm diameter, not shown) sizes of vials.

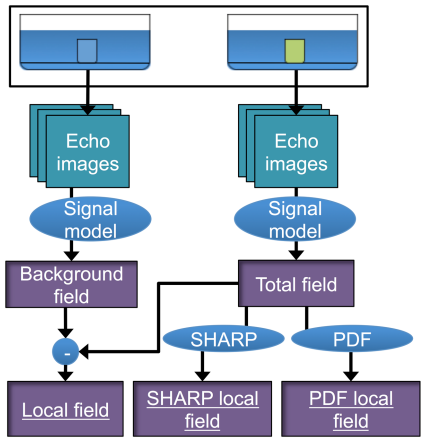

Figure 2. The flowchart shows the processing pipeline from scan data to local field estimates. The echo images were fit with a signal model to produce field maps. The noise standard deviation for PDF was estimated by the root sum of squares of the magnitude echo images.

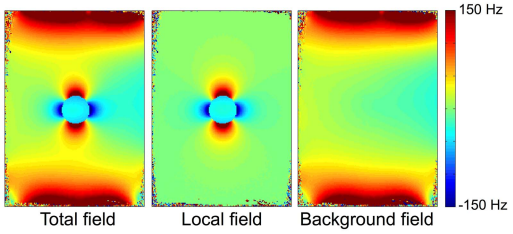

Figure 3. Acquired total field (left) for the large vial (4% Multihance) at central position shows the large inhomogeneities at the ends of the water bath. True local field (center) and background field (right) show the separation of acquired total field.

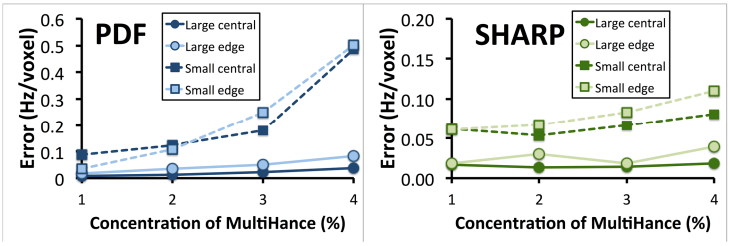

Figure 4. For both PDF and SHARP, error per voxel in the local field increases with contrast agent concentration, smaller vial size, and a closer position to air. The difference between large and small vials is much greater than the difference between central and edge positions.

References: **1.** Sharma SD et al. MRM. DOI:10.1002/ mrm.25448. **2.** Liu T et al. NMR Biomed. 2011;24:1129-36. **3.** Schweser F et al. NeuroImage. 2011;54:2789-807. **4.** Schenck JF. Med Phys. 1996;23:815-50. **5.** Zhou D et al. 3rd International Workshop on MRI Phase Contrast & Quantitative Susceptibility Mapping. 2014.

Acknowledgements: We acknowledge the support of the NIH (R01DK083380, R01DK088925, R01DK100651, UL1TR00427). We also wish to thank GE Healthcare for departmental research support.